New One-Dimensional Conductors: Graphitic Microtubules

Noriaki Hamada,[1] Shin-ichi Sawada,[1] and Atsushi Oshiyama[2]

[1]Fundamental Research Laboratories, NEC Corporation, 34 Miyukigaoka, Tsukuba 305, Japan

[2]Microelectronics Research Laboratories, NEC Corporation, 34 Miyukigaoka, Tsukuba 305, Japan

(Received 9 December 1991)

On the basis of realistic tight-binding band-structure calculations, we predict that carbon microtubules exhibit striking variations in electronic transport, from metallic to semiconducting with narrow and moderate band gaps, depending on the diameter of the tubule and on the degree of helical arrangement of the carbon hexagons. The origin of this drastic variation in the band structure is explained in terms of the two-dimensional band structure of graphite.

Recently, a new form of graphitic carbon needles has been discovered in carbon rods after an arc discharge by high-resolution transmission-electron microscopy [1]. A needle typically consists of a few microtubules centered coaxially about the needle axis, and is hollow. A microtubule has the form of a rolled graphitic sheet with a diameter of a few nanometers. Moreover, the carbon-atom hexagons on each tubule are usually arranged in a helical fashion about the needle axis. These structural characteristics are fascinating, and the condensed-matter properties of the microtubules are extremely interesting in connection with the recently discovered C_{60} solid [2].

In this Letter, we show that the graphitic microtubules exhibit a variety of properties in electronic conduction, from a typical semiconductor to a good metal, depending on the tubule structure, i.e., the diameter of the tubule and the degree of the helical arrangement. We determine the total-energy-optimized geometry for each microtubule by using Tersoff's empirical interatomic potential [3]. We then calculate band structures for a variety of total-energy-optimized microtubules by means of a reliable tight-binding method. We find a rich variation in the energy band structures of the graphitic microtubules.

There is an infinite number of possible atomic structures of the graphitic microtubules. Each structure is identified by its diameter and by the degree of the helical arrangement of the carbon hexagons. Those structures are conveniently described by choosing lattice points in a graphite sheet as follows. Suppose we have a monatomic sheet of graphite (Fig. 1). We first choose the origin and then a lattice point in the sheet. Next, we roll the sheet so that the chosen lattice point is superposed on the origin. In this way we can construct a graphite microtubule, and any microtubule, in turn, uniquely corresponds to a lattice point; i.e., we can use a lattice point of a graphite sheet as an index of the atomic structure of the graphitic microtubule. This index is denoted as $A(n_1,n_2)$ hereafter, where (n_1,n_2) represents a lattice point. In order to keep a one-to-one correspondence between the structure and the index, we confine the parameter space to $n_1 \geq 2n_2 \geq 0$. Further, after specifying (n_1,n_2) there are two ways of rolling the graphite sheet, i.e., from the back of the sheet to the front or from the front to the back.

The resulting two tubules are chiral (mirror symmetric to one another). We do not distinguish these chiral tubules in this paper, since the energy band structure that we discuss here is independent of the chiral structure. For the convenience of the discussions below, we further introduce another index: If $n_1 = l_1 n$ and $n_2 = l_2 n$, we use an index $B(l_1,l_2)n$ instead of $A(n_1,n_2)$. In this notation, (l_1,l_2) denotes a construction unit in the direction of the circumference of the tubule, and n represents the number of construction units on the circumference.

In a microtubule denoted by the above index, relaxation of carbon atoms is expected since the curvature of the tubule and thus the structural inequivalence between the axis and normal directions render the carbon-atom hexagons distorted. We determine this atomic relaxation by total-energy minimization of the carbon-atom system described by the Tersoff interatomic potential [3]. We then perform a band-structure calculation for each tubule by using a newly developed tight-binding method. The $2s$ and $2p$ orbitals of a carbon atom are used as the basis set to express the tight-binding model, and the nonorthogonality of the atomic orbitals between neighboring sites is fully taken into account. The transfer and the overlap integrals have suitable distance dependences in order to describe the band structures in various atomic configurations. The band structures of graphite and C_{60} calculated with the present tight-binding model [4] are essentially
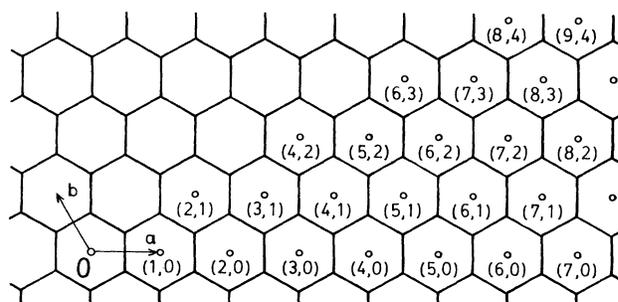

FIG. 1. A monatomic layer of graphite. Vectors a and b are unit vectors of the two-dimensional lattice. The coordinates of the lattice points are shown in the figure, which are useful to distinguish the crystal structures of tubules.

identical to those from the *ab initio* local-density calculation [5]. Technical details will be published elsewhere.

We now present several examples of the electronic band structure which clarify salient features of the graphitic microtubules. Figure 2(a) shows the geometry for the tubule $B(1,0)n$, in which a C-C bond is parallel to the tubule axis. The construction unit along the circumference is also shown in the figure. Figure 2(b) shows the first Brillouin zone (BZ) of a graphite sheet. When we make a tubule from a graphite sheet, the periodic boundary condition along the circumference allows wave vectors only on certain lines in the BZ of graphite, as shown in Fig. 2(b) (see below for further discussion). The band structure of $B(1,0)12$ is shown in Fig. 2(c). Bands higher than the Fermi level are antibonding π bands. Bonding π bands are located at energies lower than the Fermi level, while bonding $sp^2\sigma$ bands appear at energies lower than -2.5 eV and mix weakly with π bonding states. The band structure exhibits an energy gap of 8 meV at the Γ point. Figure 2(d) shows the band structure of $B(1,0)13$. In this case, the calculated energy gap is 0.697 eV. A drastic variation of the energy gap with a slight change of the tubule diameter takes place in $B(1,0)n$ tubules.

The origin of this difference in energy gap between $B(1,0)12$ and $B(1,0)13$ can be explained in terms of the two-dimensional graphite band structure. Unless the tubule diameter is extremely small, the band structure of the tubule somewhat resembles that of graphite. The main difference between graphite and the tubule lies in

the periodic boundary conditions. A graphite sheet is regarded as an infinitely extended system, and an artificial periodic boundary condition is imposed on a macroscopic scale. This results in the usual Bloch wave functions labeled with wave vectors in the first BZ. For a tubule, while the boundary condition along the tubule axis is the same as for graphite, the periodic boundary condition is imposed for a finite period along the circumference. This results in Bloch wave functions with discretely selected wave vectors. Figure 2(b) explains this situation for $B(1,0)6$. The vertical lines show the allowed wave vectors. For $B(1,0)n$, the vertical lines are found to cross the points which divide the straight line of doubled Γ-M into n parts. Of note is that the bonding and antibonding π bands are degenerate at the K point in the BZ of a graphite sheet [6]. Therefore, if a vertical line crosses the K point, namely, if n is a multiple of 3 the tubule might be a metal. However, the degenerate point is actually moved from the K point to the positions shown by open circles in Fig. 2(b), because the electron transfer is enhanced in the circumference direction due to the curvature of the tubule surface [7]. The tubule thus becomes a narrow-gap semiconductor, not a metal. Now, a rule can be derived that if n is a multiple of 3 the energy band of the tubule $B(1,0)n$ has a narrow gap, and otherwise a moderate or wide gap. This is the reason why the $B(1,0)12$ tubule has a narrow band gap and the $B(1,0)13$ tubule has a wider band gap. Figure 3 shows the calculated variation of the energy band gap as a function of n for the tubules of $B(1,0)n$, with $n = 6,7,8, \dots, 15$.

There is a special class of tubules which become metals. It is $B(2,1)n$. Figure 4(a) shows the geometry of these tubules: The tubule axis is perpendicular to a C-C bond. Figure 4(b) shows the first Brillouin zone of a graphite sheet. The set of wave vectors which are allowed by periodic boundary conditions for a tubule always contains the K point for all n, because the line crossing the Γ point always crosses the K point, as is shown in the figure. Although the enhancement of the electron transfer along the tubule circumference moves the degenerate point, the point always stays on the allowed line, as shown with
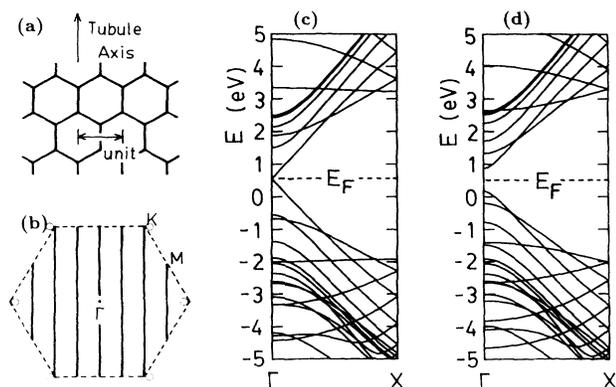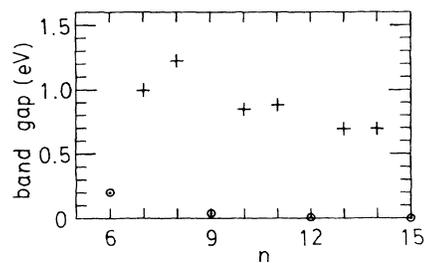

FIG. 2. (a) The geometric configuration for tubule $B(1,0)n$. "Unit" is the construction unit along the circumference, denoted by $(1,0)$. The notation $B(1,0)n$ means that the tubule has n construction units on the circumference. (b) The first Brillouin zone of a graphite sheet (the region surrounded by the dashed line), and the wave vectors allowed by the periodic boundary condition along the circumference for $n=6$ (solid lines). Open circles show the points where the bonding and the antibonding π bands are degenerate in the tubule. Band structure of (c) $B(1,0)12$ and (d) $B(1,0)13$. The X point has a wave number near π/a, with a the graphite in-plane lattice constant. Two bands stick together at the X point due to the screw symmetry.

FIG. 3. The energy band gap as a function of the number of hexagons on the circumference for tubules $B(1,0)n$. Symbols $\odot$ and $+$ represent the classes of narrow-gap and moderate-gap semiconductors, respectively.
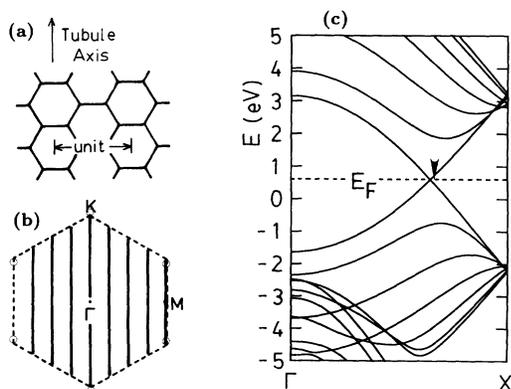
FIG. 4. (a) The geometric configuration for tubule $B(2,1)n$. (b) The first Brillouin zone of a graphite sheet (dashed line), and the wave vectors allowed by the periodic boundary condition along the circumference for $n=4$ (solid lines). Open circles show the points where the bonding and the antibonding π bands are degenerate in the tubule. (c) Band structure of $B(2,1)6$. The X point has a wave number near $\sqrt{3}\pi/a$. The arrow shows a wave vector corresponding to the K point.

open circles in Fig. 4(b). Therefore, these tubules become metallic. Figure 4(c) shows the band structure of $B(2,1)6$. Two bands cross the Fermi level at the same wave vector, exhibiting a metallic nature. The Fermi wave vector is displaced from the ideal K point shown by an arrow in the figure. The qualitative situation is unchanged for any n in $B(2,1)n$. We note that the Fermi wave vector is slightly changed with variation of the tubule diameter, namely, with varying n. Mintmire, Dunlap, and White [8] have recently shown by using a local-density band-structure calculation that the tubule of $B(2,1)5$ is metallic.

By examining the periodic boundary condition along the circumference and by referring to the energy bands of graphite, we can derive a general rule for the band gap of graphite microtubules: A tubule $A(n_1,n_2)$ $(n_1 \geq 2n_2 \geq 0)$ is (1) a metal for $n_1 - 2n_2 = 0$, (2) a narrow-gap semiconductor for $n_1 - 2n_2 = 3m$ $(m = 1, 2, \ldots)$, and (3) a moderate-gap semiconductor otherwise.

We assume in this paper that all the carbon atoms are equivalent on the tubule surface. However, a symmetry lowering due to a lattice distortion may happen at low temperatures: For example, a one-dimensional metal may suffer a Peierls distortion. Other instabilities, such as superconductivity, might be expected. The microtubule has various possibilities for the low-temperature phases.

In summary, we have systematically studied the electronic band structure of graphitic microtubules. Microtubules are categorized into three classes: The first class consists of metallic tubules, the second of semiconducting ones with narrow band gaps, and the third of semiconducting ones with moderate band gaps. The band gap is tunable by choosing the tubule structure. The graphitic microtubule is thus an extremely interesting material and a new hope for a one-dimensional conductor.

We wish to thank Dr. S. Iijima for stimulating us to calculate the electronic structure of the tubule and for fruitful discussions on the tubule structure.

[1] S. Iijima, Nature (London) 354, 56 (1991).
[2] W. Krätschmer, L. D. Lamb, K. Fostiropoulos, and D. R. Huffman, Nature (London) 347, 354 (1990).
[3] J. Tersoff, Phys. Rev. Lett. 61, 2879 (1988).
[4] N. Hamada and S. Sawada, in Proceedings of the International Workshop on Electronic Properties and Mechanisms in High-T_c Superconductors, Tsukuba, Japan, 29–31 July 1991 (Elsevier, New York, to be published).
[5] S. Saito and A. Oshiyama, Phys. Rev. Lett. 66, 2637 (1991).
[6] G. S. Painter and D. E. Ellis, Phys. Rev. B 1, 4747 (1970).
[7] The $p\pi$ atomic orbitals pointed in the radial direction are relevant for the description of the π band concerned. They are not exactly parallel but have an angle to each other, which produces an additional transfer between those orbitals, because the σ-bond components are incorporated.
[8] J. W. Mintmire, B. I. Dunlap, and C. T. White (to be published).